

Article

Analysis and Experimental Research on Vibration Reduction in Ship High-Temperature Pipeline Based on Long Coated Damping Structure

Bao Zi ¹, Feng Jiang ¹, Yiwan Wu ^{1,*} , Hongbai Bai ¹, Yu Tang ¹ and Chunhong Lu ²

¹ Engineering Research Center for Entangled Metallic Wire Materials, School of Mechanical Engineering and Automation, Fuzhou University, Fuzhou 350108, China; N190227035@fzu.edu.cn (B.Z.); N180227100@fzu.edu.cn (F.J.); bhbk@fzu.edu.cn (H.B.); 200220089@fzu.edu.cn (Y.T.)

² Department of Automotive Engineering, Hebei College of Industry and Technology, Shijiazhuang 050091, China; lchzxy2006@hbcit.edu.cn

* Correspondence: wuyiwan@fzu.edu.cn

Abstract: To reduce the vibration of a ship's high-temperature pipeline, a long coated damping structure (LCDS) with entangled metallic wire material (EMWM) is proposed in this paper. The structural analysis of the long coated damping structure for pipelines is carried out. The theoretical analysis indicates that increasing the thickness of the damping layer in a particular range can improve the vibration attenuation effect of an LCDS. Additionally, experimental verification confirms this analysis after an experimental system for pipelines. From the results, it is observed that increasing the thickness of the coated layer can effectively improve the damping property of LCDS to a certain extent. The change of the coated length and the temperature has little effect on the vibration attenuation effect of an LCDS, indicating that the LCDS can work well in a high-temperature environment.

Keywords: high-temperature pipeline; entangled metallic wire materials; damping; vibration reduction; long coated damping structure



Citation: Zi, B.; Jiang, F.; Wu, Y.; Bai, H.; Tang, Y.; Lu, C. Analysis and Experimental Research on Vibration Reduction in Ship High-Temperature Pipeline Based on Long Coated Damping Structure. *J. Mar. Sci. Eng.* **2021**, *9*, 838. <https://doi.org/10.3390/jmse9080838>

Academic Editor: José Correia

Received: 27 June 2021

Accepted: 20 July 2021

Published: 2 August 2021

Publisher's Note: MDPI stays neutral with regard to jurisdictional claims in published maps and institutional affiliations.



Copyright: © 2021 by the authors. Licensee MDPI, Basel, Switzerland. This article is an open access article distributed under the terms and conditions of the Creative Commons Attribution (CC BY) license (<https://creativecommons.org/licenses/by/4.0/>).

1. Introduction

As an essential part for transporting fuel and other fluids in ships, pipelines often vibrate due to mechanical structure excitation and internal fluid excitation. It affects the accuracy and service life of precision instruments in ships and jeopardizes workers' health.

It has been found that applying damping materials can reduce the vibration and maximize the stability of the machine. Fang et al. [1] found that coating a layer of damping material on the surface of the liquid-filled pipeline can effectively reduce the vibration and noise radiation of pipelines. Kung et al. [2] explored the relationship between the position and magnitude of constrained layer damping. Hamdaoui et al. [3] optimized the viscoelastic layer and constraint layer based on the finite element model of the constrained layer damping beam. Pilipenko et al. [4] proposed a vibration and acoustic control system for monitoring pipeline vibration. It took less time and had a low error rate. Vestrum et al. [5] studied the polymer coating pipeline by FEM (Finite Element Method), and established a constitutive model to explain the characteristics of pipeline coating material. Santi et al. [6] solved the fluid mechanics of the liquid-causing pipeline vibration in pipeline transportation by using FEM from the aspect of hydrodynamics. Kiryukhin et al. [7] studied the vibration transmission of the liquid pipeline compensator and proposed a method to reduce the vibration transmission through the joint action of structure and medium pulsation.

Researchers have found that ordinary damping materials have poor environmental adaptability and cannot be used for a long time in a high-temperature environment, which is above 200 °C. As a new type of metallic damping material, entangled metallic wire material (EMWM) has the advantages of a good corrosion resistance, long service life, and strong environmental adaptability [8,9]. EMWM is a damping material constructed of

metal wire through a series of special processes. When EMWM is subjected to an external excitation load, the internal metallic wire helices of EMWM in contact will have dry friction and dissipate energy.

In recent decades, entangled metallic wire material has been successfully applied in various fields. The researchers [10] of Texas A&M University used entangled metallic wire material to reduce the vibration of a rotor system under high-temperature and low-temperature operation and developed a metal mesh foil bearing (MMFB) shock absorber with good environmental adaptability. Lazutkin et al. [11,12] created different entangled metallic wire material specimens with the characteristics of high damping and low stiffness, which were applied to the vibration reduction in the engine pipeline system. Jiang et al. [13] studied the energy dissipation characteristics of entangled metallic wire material symmetrically coated damping structures at different temperatures and established a nonlinear energy dissipation model with temperature parameters. The model satisfactorily explains the energy dissipation characteristics of entangled metallic wire material at a high temperature of 300 °C. However, the test only verifies the low-frequency energy dissipation characteristics of the entangled metallic wire material-coated damping structure, which is still far from the vibration frequency band of the actual warship pipeline. Xiao et al. [14] designed a new type of the hanger-coated damping structure of the entangled metallic wire material for pipelines. The effects of different steam temperature, density, and the number of coated layers on the coated damping structure of the pipeline are studied. However, in his study, there is still a gap between the thermal environment simulated by steam heating and the high-temperature environment of the internal ship pipeline.

It is necessary to explore the vibration attenuation effect of entangled metallic wire material-coated damping structure at a higher temperature. The hanger-coated damping structure had small, coated areas, which could not make full use of the entangled metallic wire material' damping and energy dissipation properties. Therefore, the aim of this paper is to solve the vibration reduction problem of the high-temperature pipeline, a scheme of the long coated damping structure with entangled metallic wire material is proposed. The mechanical model is established by the method of a complex stiffness analysis. The vibration attenuation effect of the long coated damping structure is tested and verified. The effects of coated layers, coated length, and temperature on the damping property of the long coated damping structure are investigated by single factor control tests.

2. Modeling of the Long Coated Damping Structure

2.1. Long Coated Damping Structure

Figure 1 presents the scheme of the long coated damping structure (LCDS). The LCDS includes multilayer entangled metallic wire material, the pipeline, the hose clamps, and the constraining layer. A constrained damping structure is composed of the entangled metallic wire material and the constraining layer coated outside the pipeline. The traditional constrained damping structure usually uses adhesive to fix the damping layer with the base and the constraining layer. However, for entangled metallic wire material, the adhesive will make the entangled metallic wire materials unable to slide relative to the base layer and the constraining layer, which will reduce the friction energy dissipation and weaken the damping properties. Moreover, the ordinary polymer adhesive is prone to failure at high-temperature. Therefore, the scheme adopted mechanical fixation, with a thin stainless steel plate as the constraining layer and a stainless steel hose clamp as a locking device. Thus, the pipeline, the stainless steel constraining layer, and the entangled metallic wire material damping layer constitute the long coated damping structure.

Considering the length of the pipeline, to reduce the manufacturing cost, the LCDS was divided into several sections along the axial direction of the pipeline, as shown in Figure 2. Each section was coated independently according to the same preload, which the hose clamp could adjust.

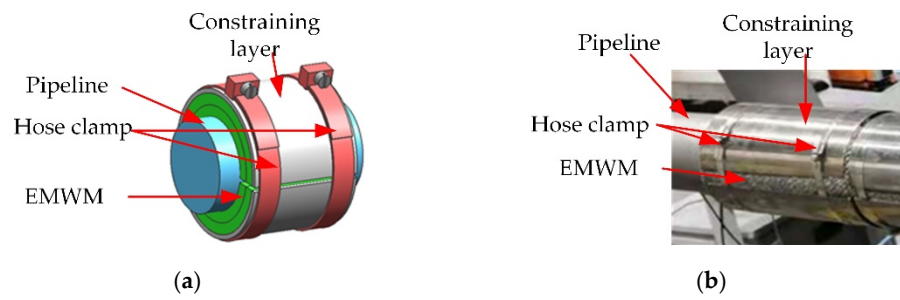


Figure 1. Scheme of the long coated damping structure. (a) schematic diagram; (b) physical picture.

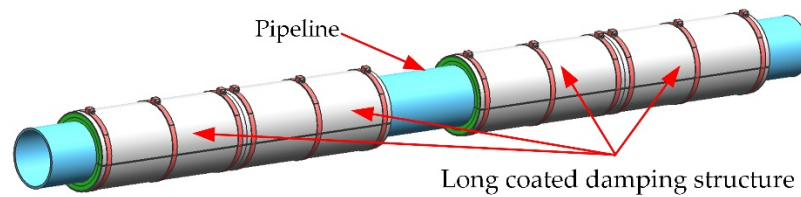


Figure 2. Scheme of segmented long coated damping structure.

2.2. Mechanical Analysis

The main theoretical analysis methods of constrained damping structures include the complex stiffness method [15], deformation energy method, fractional calculus method [16], finite element method [17], etc. The complex stiffness method is the most widely used, which derives the complex stiffness of damping structures by using the methods of material mechanics and elasticity [18,19].

According to Cravero’s research [20], to save computational resources, simple models were used to analyze the flow dynamic behavior of in turbomachinery to predict the instability operating range; these models are accurate and they can be used for the optimization strategy and to detect the vibration fluid structure. In this paper, simple pipeline models could also have been used to analyze the loss factor of LCDS to predict the damping performance. Figure 3 shows the mechanical model of the LCDS. The thickness of a thin stainless steel plate is far less than that of the entangled metallic wire material coating, which can be ignored in the analysis. Under external excitation, the LCDS produces a bending deformation. It was assumed that the pipeline had precisely the same lateral displacement as the damping layer and constraining layer, and its bending modes were also exactly the same. The ratio of the length and diameter of the pipeline was large (>10); it could be treated as a beam model. According to the Bernoulli hypothesis, the shear deformation and the moment of inertia of the section were ignored. It was assumed that the unit remained plane after the bending deformation.

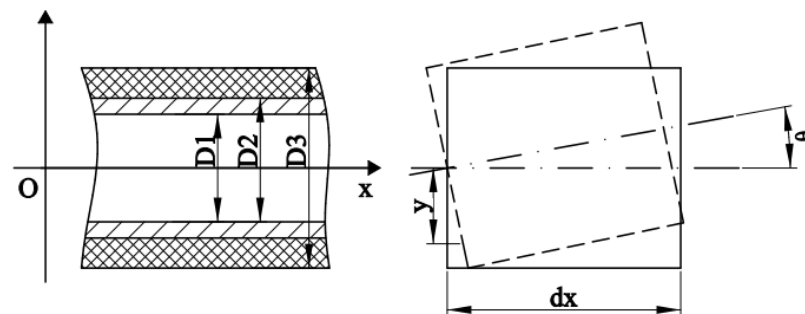


Figure 3. Mechanical model of the long coated damping structure.

As the pipeline was symmetrically arranged and the excitation point was located in the center of the pipeline, the neutral layer of the composite pipe remained unchanged.

Still, it coincided with the pipe axis during bending vibration. However, the longitudinal displacement occurred at the distance y from the neutral layer due to the rotation angle θ of the section around the neutral axis. D_1, D_2, D_3 , respectively, indicate the pipeline's inner diameter, the pipeline's outer diameter, and outer diameter of the pipeline with the damping layer.

By intercepting the micro-segment dx on the pipeline with a long coated damping structure for analysis, w is the lateral displacement, and the rotation angle θ of the section can be expressed as:

$$\theta = \frac{\partial w}{\partial x} \tag{1}$$

The longitudinal displacement can be expressed as:

$$u_y = y\theta = \frac{\partial w}{\partial x}y \tag{2}$$

The strain can be expressed as:

$$\varepsilon_y = \frac{\partial u_y}{\partial x} = y \frac{\partial^2 w}{\partial x^2} \tag{3}$$

where E_1 is the elastic modulus of the rigid pipeline and E_2 is the elastic modulus of the damping layer.

According to Hooke's law, the stress of the rigid pipe layer and damping layer can be expressed as:

$$\sigma_{y1} = E_1\varepsilon_y = E_1y \frac{\partial^2 w}{\partial x^2} \tag{4}$$

$$\sigma_{y2} = E_2\varepsilon_y = E_2y \frac{\partial^2 w}{\partial x^2} \tag{5}$$

According to the stress distribution on the section, the bending moment on the section can be expressed as:

$$M = \iint_{A_1} \sigma_{y1}y dA_1 + \iint_{A_2} \sigma_{y2}y dA_2 \tag{6}$$

From Equations (4)–(6), the bending moment on the section can be given by:

$$M = (E_1I_1 + E_2I_2) \frac{\partial^2 w}{\partial x^2} \tag{7}$$

$$I_1 = \frac{\pi}{64}(D_2^4 - D_1^4) \tag{8}$$

$$I_2 = \frac{\pi}{64}(D_3^4 - D_2^4) \tag{9}$$

where I_1 represents the moment of inertia of the pipeline, and I_2 represents the inertia of the damping layer.

From the fundamental relationship of the bending deformation, the moment M can be seen as:

$$M = B \frac{\partial^2 w}{\partial x^2} \tag{10}$$

where B is the bending stiffness of the long coated damping structure.

Setting B_1 as the bending stiffness of the pipeline, by substituting the above formula, the bending stiffness B is obtained as follows:

$$\lambda = \left(\frac{D_3^4 - D_2^4}{D_2^4 - D_1^4} \right) \tag{11}$$

$$B_1 = E_1 \frac{\pi}{64} (D_2^4 - D_1^4) \tag{12}$$

$$B = EI = E_1 I_1 + E_2 I_2 = B_1(1 + e\lambda) \tag{13}$$

where e is the elastic modulus ratio $e = E_2/E_1$.

Therefore, a complex expression of bending stiffness B_i of the i ($i = 1, 2$) layer can be expressed as:

$$B_i^* = (E_i I_i)^* = (E_i I_i)'(1 + j\eta_i) \tag{14}$$

where $(E_i I_i)'$ is the imaginary part of the bending stiffness. η_i is the cross-section loss factor of the i layer.

If the pipeline layer and constraining layer damping are ignored, the loss factor η of the long coated damping structure of the pipeline is:

$$\eta = \eta_2 \frac{e\lambda}{1 + e\lambda} \tag{15}$$

where η_2 is the loss factor of the damping layer.

Set h as the thickness of the coated layer, which is $h = D_3 - D_2$.

In the formula above, $D_1 = 96$ mm, $D_2 = 108$ mm, $E_1 = 193$ Gpa, $E_2 = 0.66$ Mpa, $\eta_2 = 0.25$. The value of η with the change of h was calculated by MATLAB. Figure 4 shows the relationship between the loss factor η and thickness h .

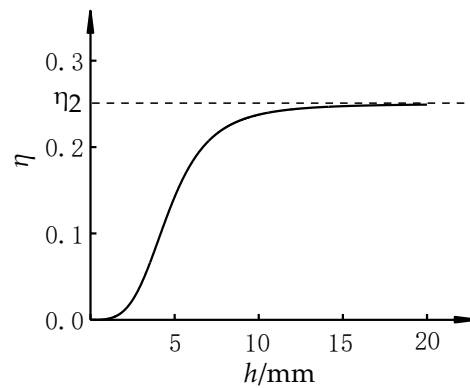


Figure 4. Relationship between η and h .

It can be seen from Figure 4 that the loss factor of the pipeline with the long coated damping structure increased with the increase in the coating thickness and gradually approached the loss factor of the damping material. It is indicated that adequately increasing the thickness of the damping layer in a particular range can increase the damping properties of the pipeline. Kartik’s research [21] found that the frequency dependency hypothesis was not shown for the EMWM loss factor results, indicating that EMWM was independent of frequency. Therefore, frequency dependence of the loss factor was not discussed here.

3. Specimen and Test Design

3.1. EMWM Specimen

In this work, a plate-like entangled metallic wire material specimen was constructed of 304 (06Cr19Ni10) austenitic stainless steel wires. For the pipeline with an outer diameter 108 mm and length 5600 mm, considering the process complexity of manufacture and installation, the entangled metallic wire material parameters were determined as $344 \times 250 \times 5$ mm. The EMWM used in LCDS was performed by CNC automatic blank winding equipment. Previous studies [22] mentioned that the influence of the winding angle on the static loss coefficient can be ignored. According to the research [22,23], the metal wire in a 45° angle with the best hook condition was generally used to prepare EMWM. Therefore, the specimen was created by the methods of previous research. The mass of the specimen was 1075 g, the density was 2.5 g/cm^3 , and the forming pressure was

1300 kN. A manufactured plate-like entangled metallic wire material specimen is shown in Figure 5.

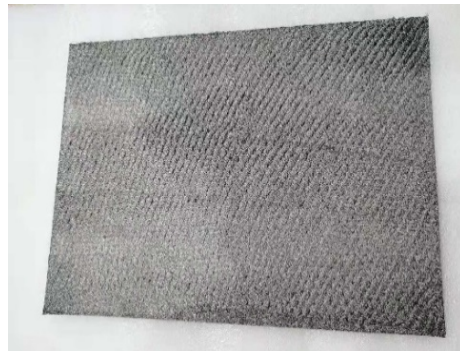


Figure 5. Plate-like entangled metallic wire material specimen.

3.2. Test System

To verify the damping performance of the pipeline with the long coated damping structure under different temperatures, a thermal–vibration joint test system for the ship pipeline was set up, as shown in Figure 6.

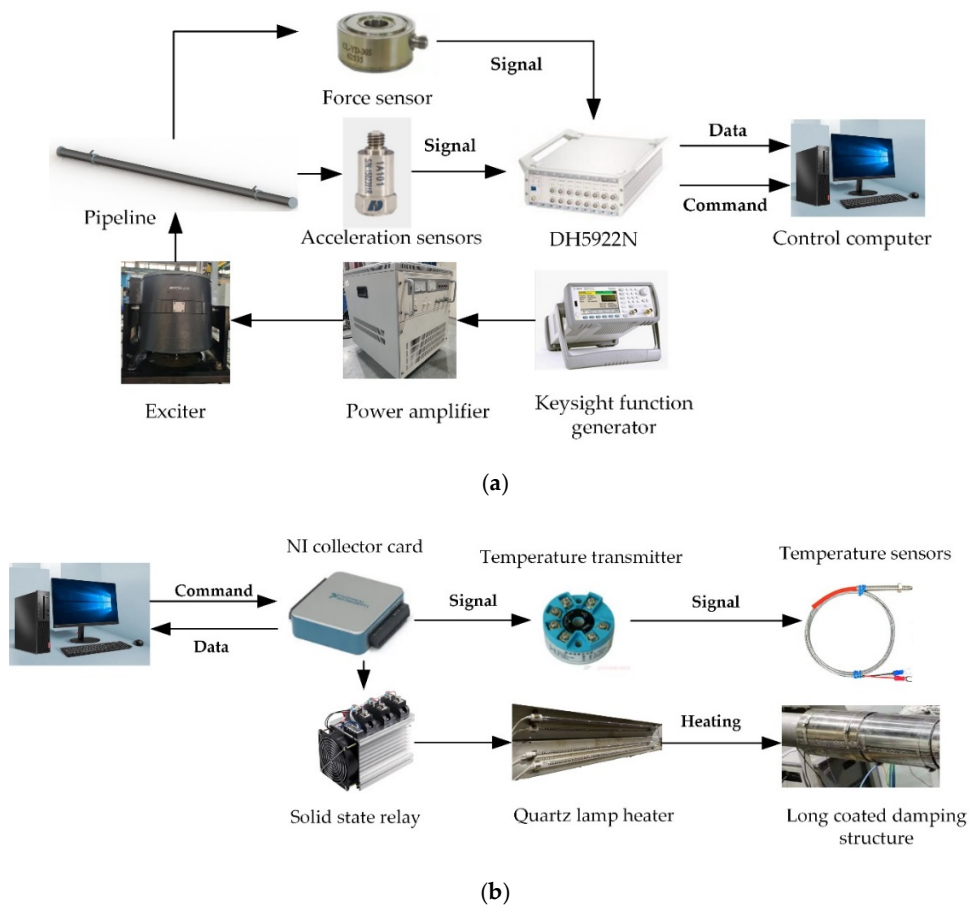


Figure 6. Block diagram of the thermal–vibration joint test system: (a) vibration excitation test system; (b) thermal environment simulation test system.

As shown in Figure 6, the vibration excitation and acquisition system was composed of two acceleration sensors, a force sensor, a multichannel data acquisition system, control computer, a power amplifier, and an electromagnetic exciter. The multichannel data acqui-

sition system was the dynamic signal acquisition system (DH5922N, Jiangsu, China). The function generator output the sine sweep signal to the power amplifier to generate an external stimulus load on the pipeline. The external stimulus load was monitored by the force sensor, which was mounted between the exciter output and the excitation rod by means of a threaded connection. The vibration signals were measured by acceleration sensors. These vibration response signals were collected in real time by DH5922N, and then they were sent to the control computer for storage and a subsequent analysis after processing.

In the thermal environment simulation test system, the pipeline was heated by quartz lamp arrays simultaneously, and the temperature was collected in real time through the temperature sensor and a high-speed data acquisition card. A host computer controlled the quartz lamp arrays based on the signal collected through the NI acquisition card and the solid-state relay. The quartz lamp arrays were controlled to turn on and off to keep the temperature of the pipeline.

Figure 7 shows the thermal–vibration joint test device for the high-temperature pipeline. The electromagnetic exciter with an elastic rope suspension was used to exert external excitation in the middle of the pipe. The vibration response of the pipeline was measured by an acceleration sensor at one hanger of the pipeline. The heat source of the thermal environment simulation test subsystem was provided by several quartz lamps. As the left and right ends of the pipeline system were centrally symmetrical, considering the cost and test convenience, the quartz lamps were installed at one end of the pipeline. After each piece of equipment was assembled, the tightening force of the electromagnetic exciter was adjusted by changing the suspension height of the exciter to ensure that the tightening force of the exciter was consistent in each test.

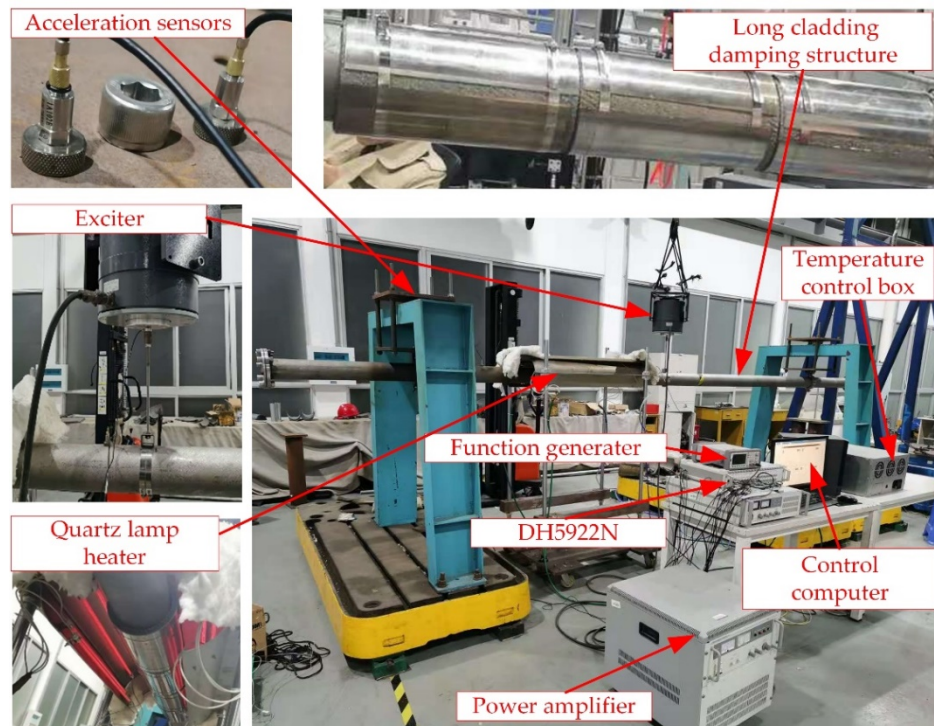


Figure 7. The thermal–vibration joint test system.

To test the temperature control performance of the heating system, a heating experiment was carried out, and the target temperature was set to 100 °C, 200 °C, and 300 °C. After reaching the target temperature, heat preservation was carried out for a period of time to ensure that the pipeline reached the target temperature [24]. Figure 8 shows the test result. Additionally, the temperature could be controlled according to the method shown in Figure 8 in the experiments.

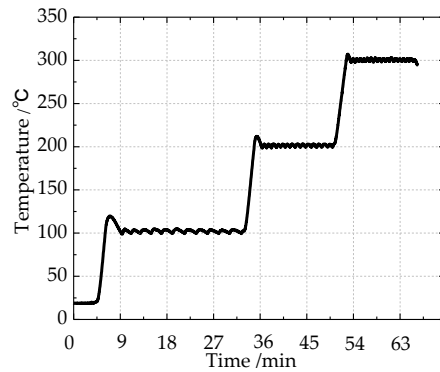


Figure 8. Relationship between heating temperature and time of pipeline.

The excitation point was located in the center of the pipeline, and the measuring point was arranged on the rigid transfer plate connected with the gantry on one side of the pipeline. The arrangement of the measuring point and the excitation point is shown in Figure 9.

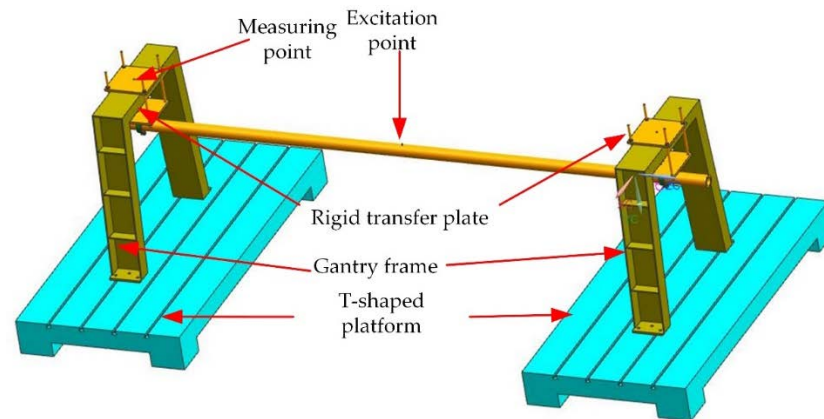


Figure 9. Arrangement of measuring points and excitation point.

4. Performance Characterization

The force transmission rate, insertion loss and vibration level difference are commonly used to evaluate the damping effect. The force transmission rate is generally used to predict the vibration isolation effect in theory, but it is not easy to measure in the experiment. Additionally, the insertion loss and the vibration level difference can be measured by the experiment. In this study, the vibration attenuation effect was evaluated by comparing the vibration response of the rigid pipeline and the pipeline with the LCDS, so the insertion loss was selected as the evaluation index of the pipeline system vibration reduction performance.

The acceleration response signal of the measuring point was collected, and the FFT transform was carried out to obtain the acceleration frequency domain response. Then, the data were processed in the following way to obtain the insertion loss of the pipeline with/without the LCDS.

Suppose there are N measuring points in a certain part of the equipment, and the acceleration response in frequency domain is $a_1(\omega), a_2(\omega), \dots, a_n(\omega)$. Then, the mean square response acceleration is as follows:

$$a_{aver}(\omega) = \sqrt{\frac{(a_1(\omega)^2 + a_2(\omega)^2 + \dots + a_n(\omega)^2)}{N^2}} \tag{16}$$

The vibration acceleration level can be expressed as:

$$L_{aver}(\omega) = 20\lg \frac{a_{aver}(\omega)}{a_0} \tag{17}$$

where a_0 is the reference acceleration, $a_0 = 10^{-6} \text{ m/s}^2$.

Suppose L_i is the vibration acceleration level at the f_i frequency point in the frequency band, and n is the total number of frequency bands for obtaining the acceleration response level in a certain frequency band. In that case the acceleration vibration level in the frequency band can be calculated by using the formula of the total vibration level octave of acceleration.

$$L_p = 10\lg \left(\frac{1}{n} \sum_{i=1}^n 10^{\frac{L_i}{10}} \right) \tag{18}$$

Based on the above formulas, the vibration levels of each frequency band can be obtained and then we can obtain the total acceleration vibration levels of each frequency band. If the whole acceleration vibration level of the rigid pipeline is L_{A0} , and the entire acceleration vibration level of the long coated damping structure is L_{A1} , the insertion loss IL of the pipeline with the LCDS can be expressed as follows:

$$IL = L_{A0} - L_{A1} \tag{19}$$

5. Results and Discussion

Before measuring the vibration attenuation effect of the long cladding damping structure, it was necessary to perform a modal analysis of the rigid pipeline for the subsequent discussion of the coating position and the analysis of the test results. The rigid pipeline, which is the pipeline without a long coated damping structure, was installed on the test system at room temperature. An electromagnetic exciter carried out the sinusoidal frequency sweep excitation from 5 Hz to 300 Hz. The vibration acceleration response curve of the rigid pipeline could be obtained by data processing of the vibration response signal monitored by the accelerometer at the measuring point. As the energy of the low-frequency resonance is more significant than that of the high-frequency resonance, the low-frequency vibration has a more substantial influence on the structure. Therefore, more attention was paid to the vibration response of the low-frequency band in the engineering. Figure 10 shows the acceleration frequency response curve of the rigid tube in 5–300 Hz, where L represents the vibration acceleration level at the measuring point. In order to obtain the modal shape of the pipeline, the finite element modal analysis (FEMA) was conducted by the finite element analysis software Abaqus®. Additionally, each mode shape of the rigid pipeline was obtained, as shown in Figure 11. It can be seen that the deformation in the middle of the pipeline was large, so it was necessary to concentrate on the middle position of the pipeline when applying the LCDS. The comparison of the natural frequency between the finite element modal analysis results and the experimental results is given to prove the accuracy of the finite element modal analysis, as shown in Table 1.

Table 1. Comparison of natural frequency between experiments and finite element model analysis (FEMA).

	Experiments	FEMA	Error
First-order	15.31 Hz	15.36 Hz	0.33%
Second-order	55.00 Hz	45.27 Hz	17.7%
Third-order	93.28 Hz	95.31 Hz	2.18%
Fourth-order	145.6 Hz	161.9 Hz	11.2%

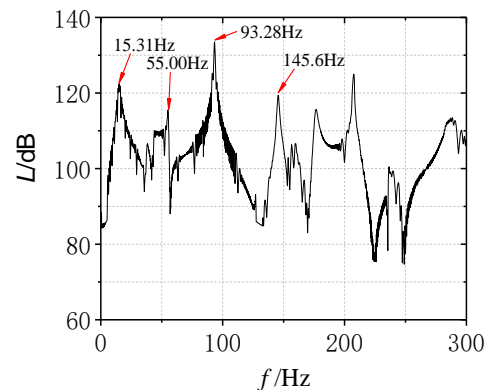


Figure 10. Vibration response of rigid pipeline.

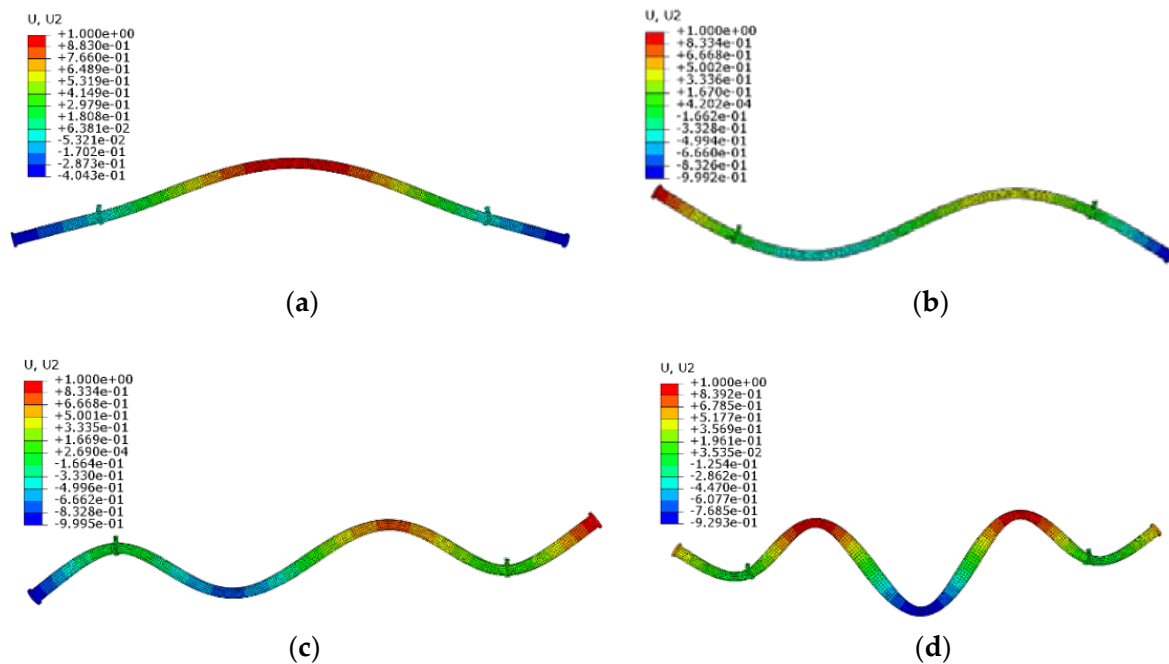


Figure 11. Modal shape of the rigid pipeline: (a) first-order modal shape; (b) second-order modal shape; (c) third-order modal shape; (d) fourth-order modal shape.

It can be seen from Table 1, the error between the test values of the second-order and fourth-order natural frequencies of the pipeline and the FEMA results was not more than 20%. The error rate between the test values of the first-order and third-order natural frequencies and the FEMA results was less than 5%. In conclusion, the natural frequencies of each order measured by the test were close to the values of FEMA, indicating that the results of the finite element modal analysis can be used for reference.

To explore the optimal position for the coating on the pipeline, eleven accelerometers were arranged on one side of the pipeline at intervals of 180 mm, starting from the center of the pipeline, as shown in Figure 12.

According to the pipeline vibration response collected by each accelerometer, the position with the maximum vibration response of the pipeline was obtained. Combined with the FEMA modal shape obtained in Figure 11 it was decided to apply the LCDS from the middle to the end of the pipeline. Additionally, the influence of the cladding position was verified by changing the cladding length in the test.

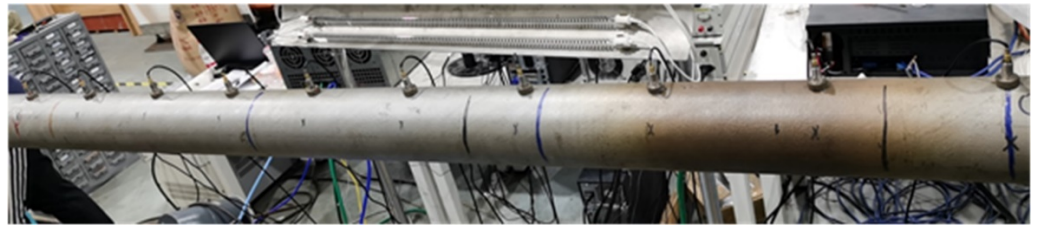


Figure 12. Vibration response of rigid pipeline.

In order to explore the influence of different ambient temperatures, different coated layers and different coated length on the vibration attenuation effect of the LCDS, the experiment was divided into three groups, as shown in Table 2.

Table 2. Three groups of parameters of long coated damping structure.

	Layers	Length (mm)	Temperature (°C)
①	1/2/3	1000	25
②	2	250/500/750/1000	25
③	2	1000	25/100/200/300

5.1. Effect of the Number of Coated Layers

An electromagnetic exciter carried out the sinusoidal frequency sweep excitation from 5 Hz to 2000 Hz. With the same ambient temperature and coated length, the experiment was carried out by changing the number of coated layers. The insertion loss value was obtained by comparing with the rigid pipeline. Additionally, the vibration attenuation effect of the LCDS was analyzed based on the insertion loss. The insertion loss of the pipeline was calculated according to Formulas (16)–(19). The test results are shown in Figures 13 and 14. It was mainly observed that the vibration attenuation effect at the first four natural frequencies formed Figure 13. As the first four natural frequencies were in the frequency band of 5–300 Hz, only the vibration response diagram of the 5–300 Hz band is given in Figure 13. Next figures of vibration response curve are based on the same principle, which will not be repeated in detail. Figure 14 shows the full-band insertion loss octave curve of 5–2000 Hz.

As shown in Figure 13, with the increase in the number of cladding layers, the total mass of the pipeline increased, but the stiffness of the pipeline changed little, while the influence on the pipeline relative to the total mass of the pipeline was negligible. The natural frequency of the object was inversely proportional to its mass so, on the whole, the natural frequency of the pipeline decreased. As shown in Table 3, with the increase in the number of EMWM layers of the LCDS, the average insertion loss of the pipeline with the LCDS in the full-band gradually increased. However, the vibration attenuation effect of the three layers was a little different from that of the double layers. With the number of coated layers increasing, the number of the internal wire helices in the contact state increased, the number of effective contact units increased, and the friction energy dissipation increased. It can be seen from Figure 14 that the insertion loss near 2000 Hz was greater than that near 5 Hz in the full band, which indicates that the vibration attenuation of the LCDS worked better in high frequencies.

To clarify the physical phenomena of the results, Figures 14 and 15 present the radial profile of the LCDS. The EMWM close to the pipeline wall had friction energy dissipation between the adjacent wire helices in the contact state and between the wire helices and the pipeline wall. The energy dissipation of the outer EMWM layer was smaller than that of the first layer. Therefore, with the increase in the number of the coated layers, the energy dissipation effect of the LCDS also increases but gradually approached the peak value. Therefore, the insertion loss of the double-layer-clad structure was greater than that of the single-layer-coated structure. However, the damping property of the LCDS with

double-layers was little different from that of the three-layers, which was consistent with the conclusion of Figure 4.

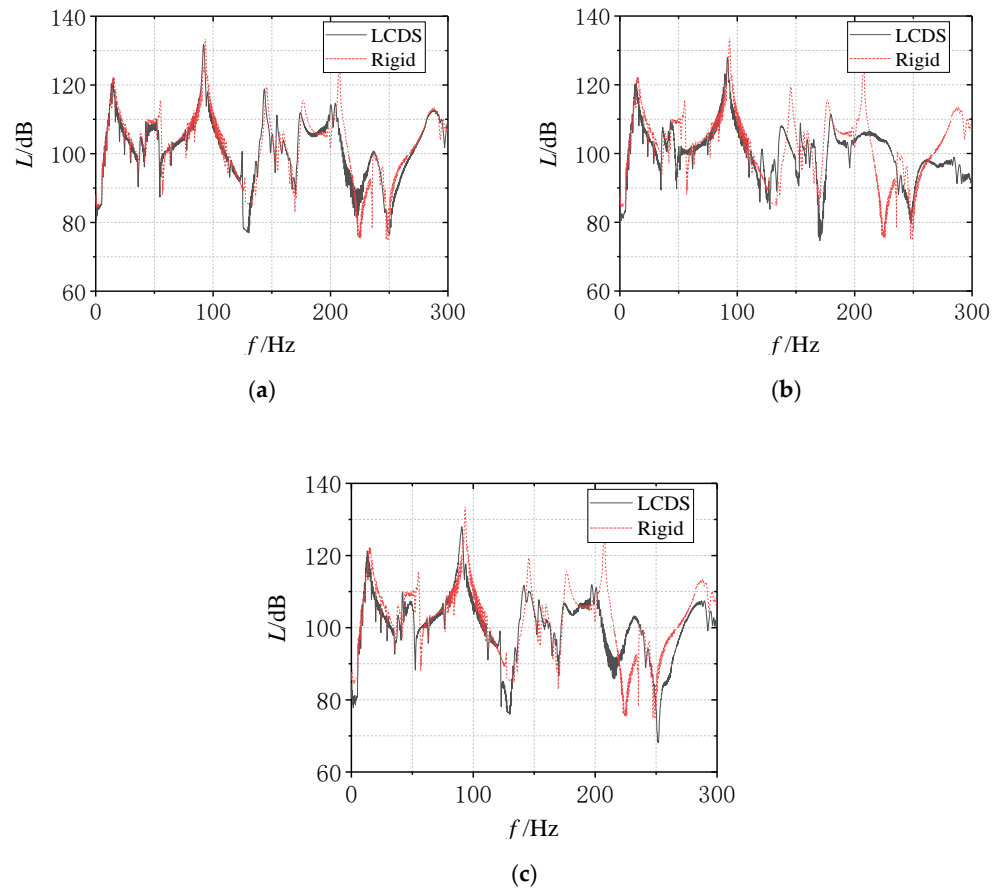


Figure 13. Vibration response curve of pipeline with different coated layers: (a) one coated layer; (b) two coated layers; (c) three coated layers.

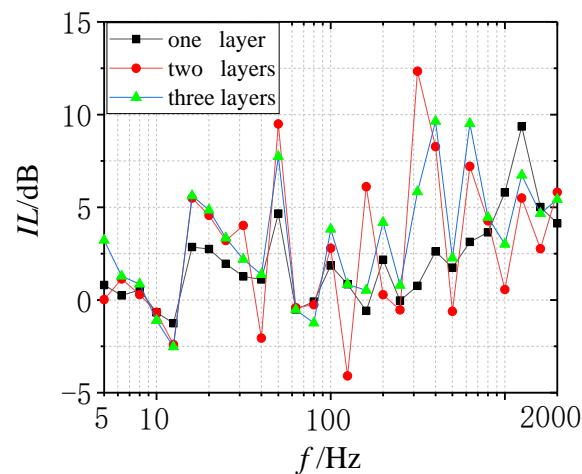


Figure 14. Insertion loss octave curves of pipeline with different coated layers.

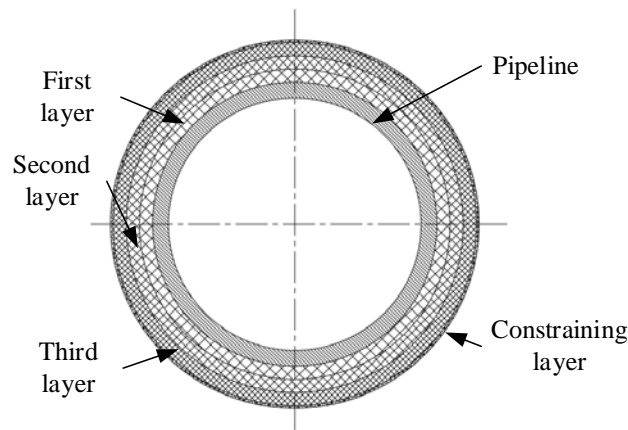


Figure 15. Profile of long coated damping structure.

Table 3. Insertion loss (IL) of pipeline with different EMWM layers (unit: dB).

Number of EMWM Layer	One	Two	Three
First-order	0.877	1.928	1.126
Second-order	6.151	5.957	5.593
Third-order	1.705	5.511	5.538
Fourth-order	0.587	11.304	7.663
Frequency range 5–2 kHz	1.719	2.559	2.970

5.2. Effect of the Temperature

An electromagnetic exciter carried out the sinusoidal frequency sweep excitation from 5 Hz to 2000 Hz. With the same coated layers and coated length, the experiment was carried out by changing the ambient temperature. The law of the change of ambient temperature in the experiment is shown in Figure 8. The insertion loss value was obtained by comparing with the rigid pipeline. Additionally, the vibration attenuation effect of the LCDS was analyzed based on the insertion loss. The insertion loss of the pipeline was calculated according to Formulas (16)–(19). The test results are shown in Figures 16 and 17. Figure 16 shows the vibration response curve in the low frequency band. Figure 17 shows the full-band insertion loss octave curve of 5–2000 Hz.

It can be seen from Figures 16 and 17 that there was little difference in the vibration response and insertion loss at different ambient temperatures, which indicates that the ambient temperature had little effect on the long coated damping structure of the pipeline. The long coated damping structure of the pipeline could still effectively reduce the vibration of the pipeline under a high-temperature environment. There was a difference in the main frequency range of energy dissipation. As shown in Table 4, the insertion loss increased at first and then decreased with the increase in ambient temperature. The maximum insertion loss value was 2.888 dB at 200 °C, and the smallest insertion loss value was 2.559 dB at room temperature. The difference between them was less than 0.5 dB, which indicates that temperature had little effect on the damping property of the LCDS.

Table 4. Insertion loss (IL) of pipeline with LCDS at different ambient temperatures (unit: dB).

Temperature	25 °C	100 °C	200 °C	300 °C
First-order	1.928	1.881	1.391	1.007
Second-order	5.957	5.975	5.318	4.614
Third-order	5.511	1.080	0.547	1.034
Fourthorder	11.31	7.787	8.285	2.524
Entire frequency range 5–2 kHz	2.559	2.600	2.889	2.563

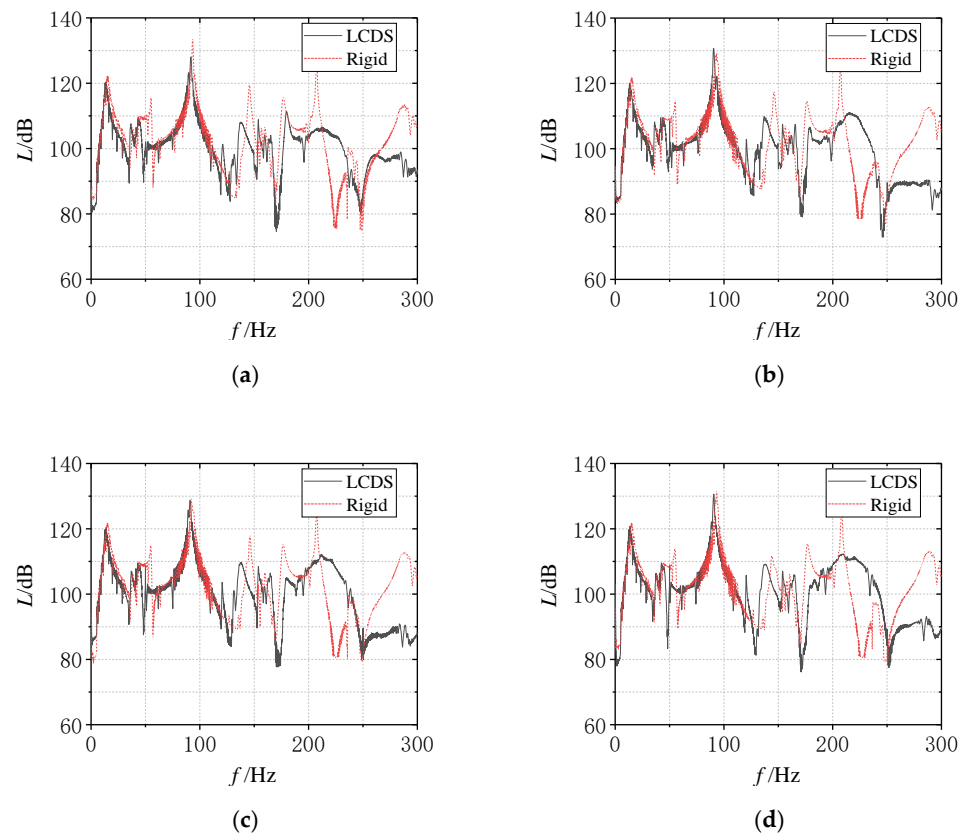


Figure 16. Vibration response curve of pipeline at different ambient temperatures: (a) 25 °C; (b) 100 °C; (c) 200 °C; (d) 300 °C.

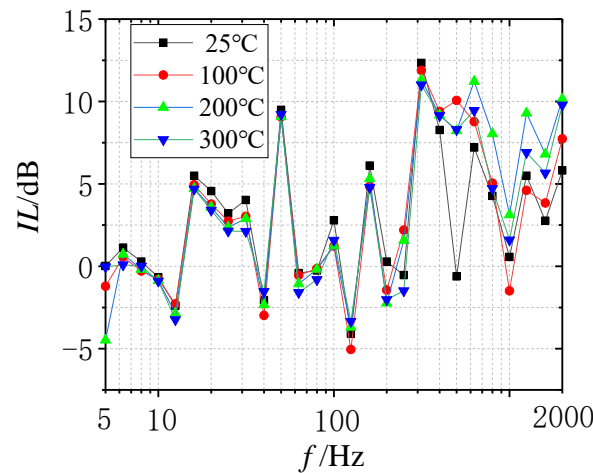


Figure 17. Insertion loss octave curves of pipeline at different ambient temperatures.

It is shown in Table 4 and Figure 17 that there was still a little difference in the insertion loss values at the corresponding modes at different temperatures. The reason why the insertion loss was lightly different at different temperatures was that the internal wire helixes of the EMWM expanded thermally with the increase in temperature. Some wire helixes transformed from the non-contact state into the slip contact state, which improved the friction energy dissipation and led to the increase in the loss factor of EMWM. When the temperature was higher than 200 °C, a dense oxide film was formed on the surface of the spiral coil, which increased the friction coefficient on the surface of the spiral coil. Additionally, the friction effect was more obvious in the high frequency, so the insertion loss at 200 °C was greater in the high frequency. However, with the increase in the ambient

temperature to 300 °C, the thermal expansion of the wire gradually increased, and the contact state of some internal wires changed from slip contact to extrusion contact, and the energy consumption slightly reduced. Overall, the temperature had little effect on the vibration attenuation effect of the LCDS.

5.3. Effect of the Length of Coated Structure

An electromagnetic exciter carried out the sinusoidal frequency sweep excitation from 5 Hz to 2000 Hz. With the same ambient temperature and coated layers, the experiment was carried out by changing the coated length. The change of the coated length meant that the LCDS was 250 mm, 500 mm, 750 mm, and 1000 mm away from the middle position of the pipeline. The insertion loss value was obtained by comparing with the rigid pipeline. Additionally, the vibration attenuation effect of the LCDS was analyzed based on the insertion loss. The insertion loss of the pipeline was calculated according to Formulas (16)–(19). The test results are shown in Figures 18 and 19. Figure 18 shows the vibration response curve in the low-frequency band. Figure 18 shows the full-band insertion loss octave curve of 5–2000 Hz.

As shown in Figures 18 and 19, the change of coated length had little influence on the pipeline system’s vibration response. The vibration attenuation effect of the smaller coated length in the low-frequency band was even better, which showed that it was unnecessary to cover the whole length of the pipeline. The location and length of damping should be determined according to the vibration distribution on the pipeline.

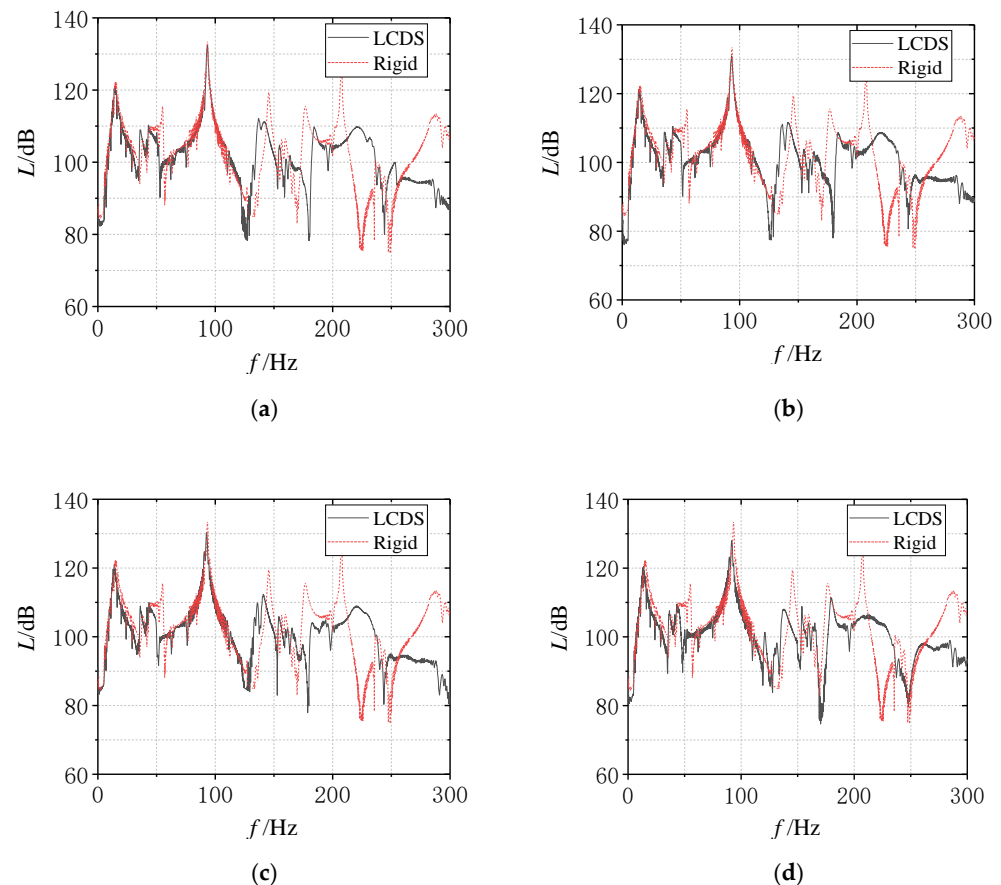


Figure 18. Vibration response curve of pipeline with different coated length: (a) 200 mm; (b) 500 mm; (c) 750 mm; (d) 1000 mm.

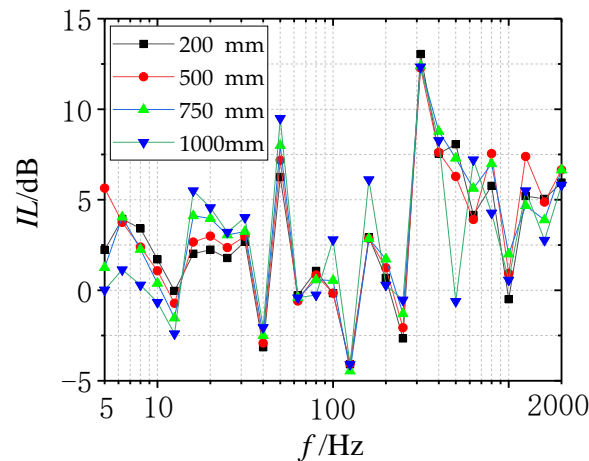


Figure 19. Insertion loss octave curves of pipeline with different coated length.

As shown in Table 5, the corresponding insertion losses of different modes under different coating lengths were various. As it can be seen from Figure 11, the mode shapes of different natural frequencies were different, and the vibration attenuation effect of different-coated length was different at different natural frequencies. It is considered that different coating lengths can give full play to their damping effect in specific modal frequencies. With the increase in the coated length of the pipeline, the insertion loss of the pipeline also increased. The increase in insertion loss meant the improvement of vibration attenuation effect of the LCDS. Compared with only coating the middle of the pipeline with EMWM and the longer length, the vibration attenuation effect was not significantly improved. From the analysis results of Figures 11 and 12, it can be seen that there was a large deformation area on both sides of the 450 mm from the center of the pipeline, and a better vibration attenuation effect could be obtained by coating this area.

Table 5. Insertion loss (IL) of pipeline with different coated length (unit: dB).

Coated Length	250 mm	500 mm	750 mm	1000 mm
First-order	1.616	1.233	1.248	1.928
Second-order	5.229	5.041	5.555	5.957
Third-order	1.023	2.564	3.176	5.511
Fourth-order	7.302	7.773	7.065	11.304
Entire frequency range 5–2 kHz	2.519	5.757	2.863	2.559

6. Conclusions

In this paper, the structural analysis for the long coated damping structure of the pipeline was carried out. It was concluded that properly increasing the thickness of the damping layer in a particular range can increase the damping effect of the long coated damping structure of the pipeline. Additionally, the rationality and accuracy of the analysis were verified by experiments.

Based on the research on the vibration reduction in the long coated damping structure of the high-temperature pipeline, according to the size of the pipeline and the existing equipment in the laboratory, the thermal–vibration joint test system was designed. The evaluation index of the insertion loss verified the vibration attenuation effect of the long coated damping structure of the pipeline. The effects of coated layers, the temperature, and coted length of the pipeline were studied. The main conclusions of experiments are as follows:

- (1) When other conditions were consistent, with the increase in the number of coated layers, the insertion loss of the pipeline increased, which improved the vibration attenuation effect of the pipeline.

- (2) With the change of temperatures, the variation of the insertion loss was less than 0.5 dB, indicating that the damping property of the LCDS could work well at high temperature.
- (3) With the increase in the coated length of the pipeline, the increase in the insertion loss was not obvious.
- (4) The loss factor of the LCDS was related to the loss factor of EMWM and the number of damping layers. Changing the number of damping layers could affect the loss factor of the LCDS.

Overall, the design of the EMWM-based LCDS can provide an effective reference for the design of the damping structure on ship pipelines working in a harsh environment.

Author Contributions: Conceptualization and methodology, B.Z., F.J., Y.W. and H.B.; data curation, B.Z., F.J. and Y.T.; validation, B.Z., F.J. and Y.W.; writing—original draft preparation, B.Z., F.J., and Y.W.; writing—review and editing, Y.W., H.B., Y.T. and C.L. All authors have read and agreed to the published version of the manuscript.

Funding: Please add: This work was supported by the National Natural Science Foundation of China (grant number 51805086) and the Natural Science Foundation of Fujian Province, China (grant number 2018J01763).

Institutional Review Board Statement: Not applicable.

Informed Consent Statement: Not applicable.

Data Availability Statement: Not applicable.

Conflicts of Interest: The authors declare no conflict of interest.

References

1. Fang, J.; Lyons, G.J. Structural damping of tensioned pipes with reference to cables. *J. Sound Vib.* **1996**, *193*, 891–907. [[CrossRef](#)]
2. Kung, S.W.; Singh, R. Vibration analysis of beams with multiple constrained layer damping patches. *J. Sound Vib.* **1998**, *212*, 781–805. [[CrossRef](#)]
3. Hamdaoui, M.; Robin, G.; Jrad, M.; Daya, E.M. Optimal design of frequency dependent three-layered rectangular composite beams for low mass and high damping. *Compos. Struct.* **2015**, *120*, 174–182. [[CrossRef](#)]
4. Pilipenko, A.E.; Rudyaga, E.V.; Kukartsev, V.V.; Tynchenko, V.S.; Kurashkin, S.O.; Rogova, D.V. A method for monitoring the violation of the integrity of pipeline communications using a radio wave vibration sensor. *IOP Conf. Ser. Mater. Sci. Eng.* **2021**, *1064*, 12023. [[CrossRef](#)]
5. Vestrum, O.; Langseth, M.; Borvik, T. Finite element analysis of porous polymer coated pipelines subjected to impact. *Int. J. Impact Eng.* **2021**, *152*, 103825. [[CrossRef](#)]
6. Maria, S.G.; Daniela, F.; Francesco, C. Effect of Coriolis Force on Vibration of Annulus Pipe. *Appl. Sci.* **2021**, *11*, 1058.
7. Kiryukhin, A.V.; Milman, O.O.; Sereshkin, L.N.; Korljakova, M.O.; Miloserdov, V.O. Physical features of fluid and structure interaction inside power unit pipeline vibration-isolating expansion joints. *J. Phys. Conf. Ser.* **2020**, *1565*, 12088. [[CrossRef](#)]
8. Hassani, V.; Tjahjowidodo, T.; Soetarto, A.D. Modeling Hysteresis with Inertial-Dependent Prandtl-Ishlinskii Model in Wide-Band Frequency-Operated Piezoelectric Actuator. *Smart Mater. Res.* **2012**, *2012*, 1–15. [[CrossRef](#)]
9. Arnaldo, M.; Leonel, P.M.; Gelman, M.; Bián, C.F.; Palacio, C.A. A Novel and Inexpensive Approach for Force Sensing Based on FSR Piezocapacitance Aimed at Hysteresis Error Reduction. *J. Sens.* **2018**, *2018*, 6561901.
10. Thomas, A.C.; Luis, S.A. Measurements of Rotordynamic Response and Temperatures in a Rotor Supported on Metal Mesh Foil Bearings. *J. Eng. Gas Turbines Power* **2013**, *135*, 122507.1–122507.10.
11. Lazutkin, G.V.; Ermakov, A.I.; Davydov, D.P.; Boyarov, K.V.; Bondarchuk, P.V. Analysis of characteristics of all-metal vibration insulators made of different wire materials. *Russ. Aeronaut.* **2014**, *57*, 327–332. [[CrossRef](#)]
12. Lazutkin, G.V.; Boyarov, K.V.; Davydov, D.P.; Volkova, T.V.; Varzhitskii, L.A. Design of Elastic-damping Supports Made of MR Material for Pipeline Supports. *Procedia Eng.* **2017**, *176*, 326–333. [[CrossRef](#)]
13. Jiang, F.; Ding, Z.; Wu, Y.; Bai, H.; Shao, Y.; Zi, B. Energy Dissipation Characteristics and Parameter Identification of Symmetrically Coated Damping Structure of Pipelines under Different Temperature Environment. *Symmetry* **2020**, *12*, 1283. [[CrossRef](#)]
14. Xiao, K.; Bai, H.; Xue, X.; Wu, Y.; Tusset, A.M. Damping Characteristics of Metal Rubber in the Pipeline Coating System. *Shock Vib.* **2018**, *2018*, 3974381. [[CrossRef](#)]
15. Teng, T.; Hu, N. Analysis of damping characteristics for viscoelastic laminated beams. *North-Holland* **2001**, *190*, 3881–3892. [[CrossRef](#)]
16. Bagley, R.L.; Torvik, P.J. Fractional calculus in the transient analysis of viscoelastically damped structures. *AIAA J.* **1985**, *23*, 918–925. [[CrossRef](#)]

17. Wang, Y. Finite element analysis and experimental study on dynamic properties of a composite beam with viscoelastic damping. *J. Sound Vib.* **2013**, *332*, 6177–6191. [[CrossRef](#)]
18. Mead, D.J. The measurement of the loss factors of beams and plates with constrained and unconstrained damping layers: A critical assessment. *J. Sound Vib.* **2006**, *300*, 744–762. [[CrossRef](#)]
19. Aenlle, M.L.; Pelayo, F. Frequency Response of Laminated Glass Elements: Analytical Modeling and Effective Thickness. *Appl. Mech. Rev.* **2013**, *65*, 020802. [[CrossRef](#)]
20. Cravero, C.; Davide, M. Criteria for the Stability Limit Prediction of High Speed Centrifugal Compressors with Vaneless Diffuser: Part I—Flow Structure Analysis. Turbo Expo: Power for Land, Sea, and Air. *Am. Soc. Mech. Eng.* **2020**, *84102*, V02ET39A013.
21. Kartik, C.; Jem, R.; Elizabeth, C. Mechanical behavior of tangled metal wire devices. *Mech. Syst. Signal Process.* **2019**, *118*, 13–29.
22. Jianwen, Z. Preparation Process and Performance Analysis of Metal Rubber with Large-Size Flat Plate with Holes. Master's Thesis, Fuzhou University, Fuzhou, China, 2019.
23. Hui, C. Winding Crafts and Equipment Researching of Metal Rubber. Master's Thesis, Xi'an Technological University, Xi'an, China, 2014.
24. Ding, Z.; Bai, H.; Wu, Y.; Zhu, Y.; Shao, Y. Experimental Investigation of Thermal Modal Characteristics for a Ship's Foundation under 300 °C. *Shock Vib.* **2019**, *2019*, 2714930. [[CrossRef](#)]